Journal of Engineering Physics and Thermophysics, Vol. 72, No. 4, 1999

EFFECTIVE ABSORPTION COEFFICIENT OF A SELECTIVE MEDIUM WITHIN A FINITE SPECTRAL RANGE WITH REGARD FOR SCATTERING

M. L. German, D. Lempert, V. P. Nekrasov, E. F. Nogotov, and S. Rozin

UDC 536.34:535.36

The effect of scattering on the lineshape of outgoing radiation for the regular absorption band model is investigated for the model of a homogeneous plane-parallel radiating, absorbing, and scattering layer with transparent boundaries. The investigation is based on numerical solution of the integrodifferential equation of radiation transport. Based on an analysis of results obtained, methods more accurate than the known ones are proposed for calculation of the absorption coefficient by a selective component of the medium averaged over a finite spectral range.

Introduction. Investigation of the mechanism of the radiation transport in two-phase (gas + solid particles) media is important for solving a number of scientific and practical problems such as, e.g., radiative and complex heat transfer, neutron transport in nuclear reactors, direct and inverse problems of the spectroscopy of scattering media, propagation of radiation in the atmosphere, etc. Accurate calculations for scattering processes in two-phase media with regard for selective properties of gas components are of special interest. It has been shown in [1-5] that these processes can lead in a number of cases to a change in the lineshape of the outgoing radiation.

The accuracy of calculations of radiation transport in nonhomogeneous, nonisothermal, and nonequilibrium gas media based on solution of the integrodifferential transport equation substantially depends on the accuracy of input optical and thermodynamic parameters of the medium. Accurate calculations for the H_2O, CO, CO_2, and NO_x molecules require taking into account hundreds to thousands of spectral lines lying within the range of $1-10$ μm whose parameters are nonlinear functions of the temperature and pressure. In the literature, this method is known as the line-by-line method [6, 7]. It is extremely painstaking and is hardly suitable for practical calculations. Mainly, it is recommended for evaluating the accuracy of solutions obtained based on various approximate models used for description of actual gas spectra.

The narrow-band approximation [8, 9] and the model of the weighted sum of gray gases [10] are most frequently used in calculations of the transmission of the medium within a given spectral range. It should be noted that in this case, certain difficulties with evaluating the total absorption coefficient arise in calculations of the propagation of radiation in nonhomogeneous, nonisothermic, and nonequilibrium gas media with regard for scattering based on solving the integrodifferential transport equation. Extensive investigations on obtaining the model absorption coefficient of radiating gases that would approximate to a given accuracy the actual absorption coefficient within a particular spectral range are presently carried out [10, 11].

The present work is devoted to solution of the above problem. It provides more accurate methods compared to known ones suitable for calculation of the absorption by a gas component of the absorbing medium within a finite spectral range. Presented in what follows are results concerning the regular model of the Lorentzian-shaped Elsasser absoption band.

Effect of Scattering on the Lineshape of Outgoing Radiation. The dependence of the lineshape of outgoing radiation on scattering processes is investigated based on the model of a plane-parallel homogeneous radiating layer

Academic Scientific Complex "A. V. Luikov Institute of Heat and Mass Transfer" of the National Academy of Sciences of Belarus, Minsk, Belarus; Ben-Gurion University, Beersheba, Israel. Translated from Inzhenerno-Fizicheskii Zhurnal, Vol. 72, No. 4, pp. 728-735, July-August, 1999. Original article submitted December 1, 1998.

 1062-0125/99/7204-0702$22.00

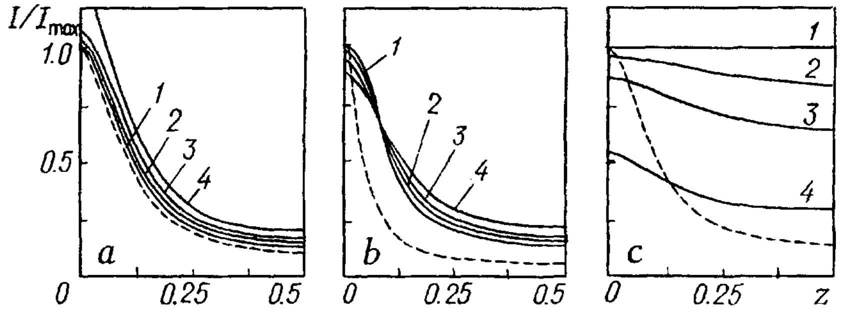

Fig. 1. Distribution of the radiation intensity of the medium across the absorption line (dashed line) for $\gamma/d = 0.1$, $\tau_a = 0.1$ (a); $\gamma/d = 0.05$, $\tau_a = 0.5$ (b); $\gamma/d = 0.1$, $\tau_a = 50$ (c), and $Sc_a = 0$ (1), 0.3 (2), 0.6 (3), and 0.9 (4).

with transparent boundary surfaces. The investigation is based on the numerical solution of the integrodifferential equation of radiative transport [12]. The scattering anisotropy is taken into account within the transport approximation [13]. In this case, the radiative transport equation can be written as follows:

$$m \frac{dI(m, l)}{dl} + (\chi + a\sigma) I(m, l) = \frac{a\sigma}{2} \int_{-1}^{1} I(m', l)\, dm' + \chi B(\tau). \tag{1}$$

We also introduce the Schuster number $Sc = a\sigma/(\chi + a\sigma)$ and the optical layer thickness with respect to absorption $\tau = \chi L$.

Radiation of molecular gases within a finite spectral range is modeled by a set of equidistantly spaced Lorentzian-shaped lines with identical intensities. In this case the optical thickness of the gas layer is as follows:

$$\tau(z, \gamma/d, sL/d) = \frac{sL}{d} \frac{\sinh(2\pi\gamma/d)}{\cosh(2\pi\gamma/d) - \cos(2\pi z)} = \tau_a \zeta(\gamma/d, z)). \tag{2}$$

We also introduce the gray optical layer thickness with respect to absorption $\tau_a = sL/d$ and the gray Schuster number $Sc_a = a\sigma/(a\sigma + s/d)$.

Results of the numerical solution of Eq. (1) with regard for integration of the absorption coefficient over the frequency (2) within the range of $-0.5 < z < 0.5$ are presented in Fig. 1 for different parameters of the fine structure of the line. The curves presented illustrate the dependence of the intensity of radiation outgoing from the layer normally to the boundary surface on processes of scattering on particles. As is easily seen, the dependence is rather complex. The scattering affects both the lineshape and intensity of outgoing radiation.

For weak narrow lines, the intensity of outgoing radiation increases both in the center and at the wings with the Schuster number (Fig. 1a). As the line becomes stronger, the inetnsity of radiation starts to increase at the wings and to decrease in the center (Fig. 1b). For strong lines, the gas radiation outgoing from the layer has a uniform lineshape. Selective properties of gases reveal themselves with an increasing Schuster parameter, since the radiation intensity first decreases at the line edges and then in the center due to the scattering (Fig. 1c).

An analysis of the data presented shows that integration over the frequency is required in calculations of radiation of selectively emitting gases and scattering parameters, since the Schuster parameter varies within the limits of the emission line. However, when carrying out extensive calculations, this leads to a substantial increase in the CPU time. A separate consideration of scattering and absorption processes can lead, as is shown by practical computations, to uncontrollable errors.

We introduce the quantity referred to in what follows as the optical thickness of the selective component averaged over the lineshape $\tau_0 = \tau(\gamma/d, \tau_a, Sc_a)$, which satisfies the identity

$$I(\tau_0, Sc_a) = \int_{-0.5}^{0.5} I(z, \gamma/d, \tau_a, Sc_a)\, dz. \tag{3}$$

Dependences $\tau_0(Sc_a)$ obtained by solving Eq. (3) are presented in Fig. 2. The data presented show that the quantity τ_0 can decrease (Fig. 2a) or increase (Fig. 2b) with the Schuster number, or have an extremum (Fig. 2c), depending

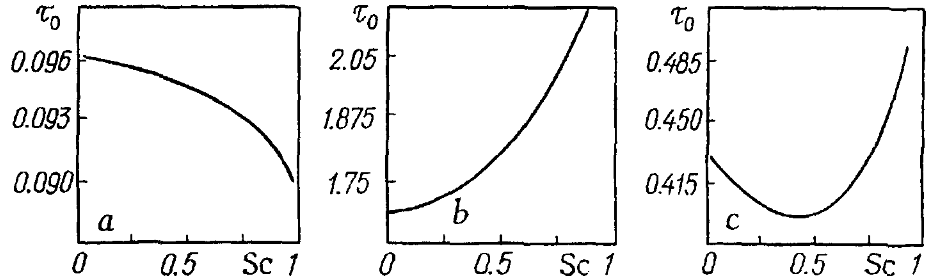

Fig. 2. Effect of the gray Schuster number on the mean optical thickness for the lineshape with $\gamma/d = 0.1$, $\tau_a = 0.1$ (a), $\gamma/d = 0.1$, $\tau_a = 3.0$ (b), and $\gamma/d = 0.01$, $\tau_a = 3.0$ (c).

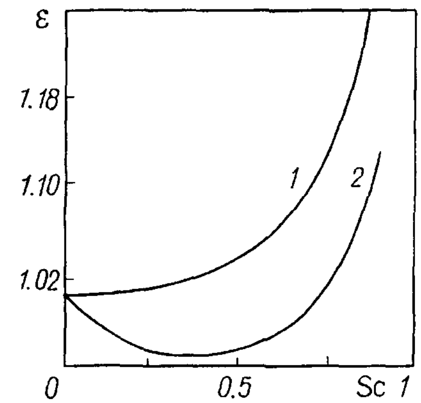

Fig. 3. Errors due to neglecting the effect of scattering processes on the absorption lineshape for $\gamma/d = 0.1$ and $\tau_a = 3.0$ (1) and 0.01 (2).

on the values of the fine structure parameters. The quantity varies over a rather wide range, and it can vary by several hundred percent.

Further, we introduce into consideration the quantity $\varepsilon = I(\tau_1, 0)/I(\tau_2, \mathrm{Sc_a})$ – the ratio of the emissivity of the medium within a finite spectral range with regard for the scattering effect on the lineshape of the outgoing radiation to the same parameter evaluated neglecting the effect of the scattering fraction on the lineshape-averaged optical thickness of the selective component. Here $\tau_1 = \tau_0(\gamma/d, \tau_a, \mathrm{Sc_a} = 0)$ is the average optical thickness of the selective component for the nonscattering medium and $\tau_2 = \tau_0(\gamma/d, \tau_a, \mathrm{Sc_a})$ is that for the scattering medium. The quantity ε charactererizes errors due to ignorance of the effect of scattering processes on the lineshape-averaged optical thickness of the selective component. The dependence of ε on the value of the Schuster number for different parameters of the absorption line is illustrated by the curves presented in Fig. 3.

Average Absorption Coefficient for Elsasser's Model. An analysis of computational results obtained in the preceding section has shown that scattering substantially affects the intensity of a selectively emitting medium. However, the direct integration of the radiative transport equation over the lineshape is, as has been noted above, time-consuming, especially in the case of computations within a wide spectral range (1–8 μm). Moreover, Elsasser's model frequently does not yield an exact value for emission of gases with actual specta.

An effective absorption coefficient that would account for parameters of the fine structure of the emission line and would not require frequency integration is required for extensive computations of radiation in scattering media. Let us present the average absorption coefficient in the following form:

$$K = \frac{S}{d} \xi (\gamma/d, \tau_a) . \tag{4}$$

The correction factor for the absorption lineshape upon radiation transport in the nonscattering medium is defined as follows:

TABLE 1. Correction Factor $\xi(\gamma/d, \tau_a)$ for Elsasser's Model ($\chi = \xi s/d$)

τ	γ/d												
	0.001	0.002	0.005	0.007	0.010	0.025	0.050	0.075	0.100	0.175	0.250	0.375	0.500
0.0001	0.986	0.992	0.994	0.995	0.996	0.998	0.999	1.000	1.000	1.000	1.000	1.000	1.000
0.0002	0.979	0.989	0.993	0.995	0.995	0.998	0.998	0.999	1.000	1.000	1.000	1.000	1.000
0.0003	0.972	0.986	0.991	0.993	0.995	0.997	0.998	0.999	0.999	1.000	1.000	1.000	1.000
0.0004	0.964	0.983	0.990	0.992	0.994	0.997	0.998	0.999	0.999	0.999	1.000	1.000	1.000
0.0005	0.957	0.980	0.988	0.991	0.993	0.997	0.998	0.999	0.999	1.000	1.000	1.000	1.000
0.0006	0.950	0.977	0.987	0.991	0.992	0.996	0.998	0.999	0.999	1.000	1.000	1.000	1.000
0.0007	0.943	0.974	0.985	0.989	0.992	0.996	0.998	0.999	0.999	1.000	1.000	1.000	1.000
0.0008	0.936	0.971	0.984	0.988	0.991	0.996	0.998	0.998	0.999	1.000	1.000	1.000	1.000
0.0009	0.929	0.968	0.982	0.987	0.990	0.995	0.998	0.999	0.999	1.000	1.000	1.000	1.000
0.0010	0.923	0.965	0.981	0.987	0.989	0.995	0.998	0.998	0.999	1.000	1.000	1.000	1.000
0.0020	0.861	0.937	0.966	0.977	0.982	0.992	0.996	0.998	0.999	0.999	1.000	1.000	1.000
0.0030	0.808	0.911	0.952	0.967	0.975	0.990	0.995	0.997	0.998	0.999	1.000	1.000	1.000
0.0040	0.761	0.886	0.939	0.958	0.968	0.987	0.994	0.997	0.998	0.999	1.000	1.000	1.000
0.0050	0.720	0.863	0.926	0.949	0.961	0.985	0.993	0.996	0.997	0.999	1.000	1.000	1.000
0.0060	0.684	0.840	0.913	0.940	0.954	0.982	0.992	0.995	0.997	0.999	1.000	1.000	1.000
0.0070	0.652	0.819	0.900	0.931	0.948	0.979	0.991	0.995	0.997	0.999	1.000	1.000	1.000
0.0080	0.624	0.800	0.888	0.923	0.941	0.977	0.990	0.994	0.996	0.999	1.000	1.000	1.000
0.0090	0.599	0.781	0.876	0.914	0.935	0.974	0.989	0.993	0.996	0.999	0.999	1.000	1.000
0.0100	0.576	0.763	0.865	0.906	0.928	0.972	0.987	0.993	0.995	0.999	0.999	1.000	1.000
0.0200	0.431	0.626	0.766	0.831	0.869	0.947	0.976	0.987	0.992	0.997	0.999	1.000	1.000
0.0300	0.358	0.539	0.690	0.769	0.817	0.924	0.966	0.980	0.988	0.996	0.999	1.000	1.000
0.0400	0.312	0.478	0.630	0.717	0.772	0.901	0.955	0.974	0.984	0.995	0.998	1.000	1.000
0.0500	0.281	0.434	0.582	0.672	0.732	0.880	0.945	0.968	0.980	0.994	0.998	1.000	1.000
0.0600	0.257	0.399	0.543	0.634	0.697	0.860	0.935	0.962	0.976	0.992	0.997	0.999	1.000
0.0700	0.239	0.372	0.510	0.601	0.666	0.841	0.925	0.957	0.972	0.991	0.997	0.999	1.000
0.0800	0.224	0.350	0.482	0.572	0.638	0.823	0.916	0.951	0.969	0.990	0.996	0.999	1.000
0.0900	0.211	0.331	0.459	0.547	0.613	0.806	0.906	0.945	0.965	0.989	0.996	0.999	1.000
0.1000	0.201	0.315	0.438	0.525	0.590	0.789	0.897	0.940	0.961	0.988	0.995	0.999	1.000
0.2000	0.143	0.227	0.320	0.390	0.447	0.661	0.816	0.887	0.926	0.976	0.991	0.998	1.000
0.3000	0.117	0.187	0.265	0.325	0.375	0.577	0.752	0.842	0.894	0.964	0.987	0.997	0.999
0.4000	0.102	0.163	0.232	0.285	0.330	0.519	0.699	0.802	0.865	0.953	0.982	0.996	0.999
0.5000	0.092	0.146	0.209	0.257	0.298	0.476	0.656	0.767	0.838	0.942	0.978	0.995	0.999
0.6000	0.084	0.134	0.192	0.237	0.275	0.442	0.620	0.736	0.813	0.931	0.974	0.995	0.999
0.7000	0.078	0.125	0.178	0.221	0.257	0.416	0.590	0.708	0.791	0.921	0.970	0.994	0.999
0.8000	0.073	0.117	0.168	0.208	0.242	0.394	0.565	0.684	0.770	0.911	0.965	0.993	0.999
0.9000	0.069	0.110	0.159	0.197	0.230	0.376	0.542	0.662	0.751	0.902	0.961	0.992	0.998
1.0000	0.065	0.105	0.151	0.188	0.219	0.360	0.523	0.643	0.734	0.892	0.957	0.991	0.998
2.0000	0.047	0.076	0.110	0.138	0.162	0.274	0.412	0.524	0.618	0.817	0.921	0.982	0.996
3.0000	0.039	0.063	0.092	0.116	0.136	0.235	0.360	0.465	0.556	0.765	0.890	0.974	0.994
4.0000	0.034	0.055	0.081	0.102	0.121	0.211	0.329	0.429	0.518	0.728	0.865	0.966	0.993
5.0000	0.030	0.050	0.074	0.093	0.111	0.195	0.308	0.405	0.491	0.701	0.844	0.959	0.991
6.0000	0.028	0.046	0.068	0.087	0.103	0.184	0.292	0.386	0.471	0.681	0.827	0.952	0.989
7.0000	0.026	0.043	0.064	0.082	0.097	0.174	0.280	0.372	0.456	0.665	0.813	0.946	0.987
8.0000	0.025	0.041	0.061	0.077	0.092	0.167	0.270	0.361	0.444	0.652	0.802	0.940	0.986
9.0000	0.023	0.039	0.058	0.074	0.089	0.161	0.262	0.352	0.434	0.641	0.792	0.934	0.984
10.0000	0.022	0.037	0.056	0.071	0.085	0.156	0.255	0.344	0.425	0.631	0.783	0.929	0.982
20.0000	0.016	0.028	0.043	0.056	0.067	0.129	0.219	0.302	0.380	0.582	0.737	0.897	0.969
30.0000	0.014	0.024	0.037	0.049	0.060	0.117	0.204	0.285	0.361	0.562	0.717	0.881	0.959
40.0000	0.012	0.021	0.034	0.045	0.055	0.111	0.195	0.275	0.351	0.550	0.705	0.871	0.953
50.0000	0.011	0.020	0.031	0.042	0.052	0.106	0.190	0.269	0.344	0.543	0.698	0.864	0.948
60.0000	0.010	0.019	0.030	0.040	0.050	1.103	0.186	0.264	0.339	0.537	0.692	0.860	0.945
70.0000	0.010	0.018	0.029	0.038	0.048	0.100	0.182	0.260	0.335	0.533	0.688	0.856	0.942
80.0000	0.009	0.017	0.028	0.037	0.047	0.099	0.180	0.258	0.332	0.530	0.685	0.853	0.940
90.0000	0.009	0.016	0.027	0.036	0.045	0.097	0.178	0.255	0.329	0.527	0.682	0.851	0.938
100.0000	0.009	0.016	0.026	0.035	0.044	0.096	0.176	0.253	0.327	0.525	0.680	0.849	0.936
200.0000	0.007	0.013	0.022	0.031	0.040	0.089	0.167	0.244	0.317	0.514	0.670	0.840	0.929
300.0000	0.006	0.012	0.021	0.029	0.037	0.086	0.164	0.240	0.313	0.510	0.665	0.836	0.926
400.0000	0.006	0.011	0.020	0.028	0.036	0.084	0.162	0.238	0.311	0.507	0.663	0.834	0.924
500.0000	0.005	0.011	0.019	0.027	0.035	0.083	0.161	0.236	0.309	0.506	0.662	0.833	0.923
600.0000	0.005	0.010	0.019	0.027	0.035	0.082	0.160	0.236	0.309	0.505	0.661	0.832	0.922
700.0000	0.005	0.010	0.018	0.026	0.034	0.082	0.159	0.235	0.308	0.504	0.660	0.831	0.921

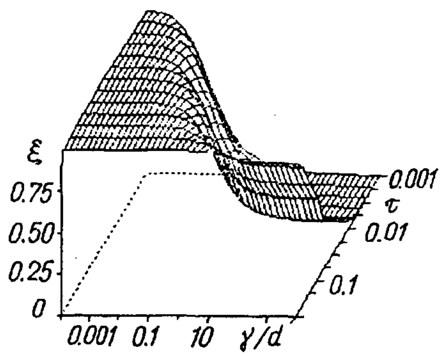

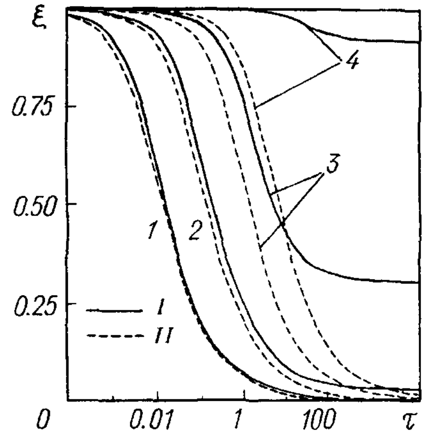

Fig. 4. Distribution of the correction coefficient $\xi(\gamma/d, \tau)$.

Fig. 5. Dependence of the correction factor ξ on the optical thickness τ for γ/d = 0.001 (1), 0.01 (2), 0.1 (3), and 0.5 (4); *I*, exact solution and *II*, approximating formula (6).

$$\xi(\gamma/d, \tau_a) = -\frac{1}{\tau_a}\int_{-0.5}^{0.5} \exp(-\tau_a \zeta(\gamma/d, z))\, dz\,. \tag{5}$$

Table 1 and Fig. 4 present values of $\xi(\gamma/d, \tau_a)$ obtained by numerical integration of Eq. (1) with an accuracy of 0.0001% for the ranges of the parameters $10^{-4} \le \tau_a \le 10^4$ and $0.001 \le \gamma/d \le 0.5$. In what follows, we will refer to these as the exact values. An analysis of the behavior of the function $\xi(\gamma/d, \tau_a)$ shows that it is rather smooth and has no extrema. At γ/d = const, it decreases with increasing τ_a, and at τ_a = const, it increases with γ/d. This function has the following asymptotes:

1. $\lim\limits_{\tau\to 0} \xi(\gamma/d, \tau_a) = 1$ (in practice, at $sL/\gamma < 0.01$);

2. $\lim\limits_{\tau\to 0} \xi(\gamma/d, \tau_a) = \dfrac{\sinh(2\pi\gamma/d)}{\cosh(2\pi\gamma/d) + 1} = \zeta_{min} < 1$.

Presently, the following formula is most frequently recommended for calculating the correction factor ξ [2]:

$$\xi_1(\gamma/d, \tau) = \frac{1}{\sqrt{1 + 0.25\tau\gamma/d}}\,. \tag{6}$$

However, its use leads to substantial errors for both the quantity ξ (up to 100%) and the averaged intensity of the outgoing radiation $\varepsilon = 1 - I(\xi_1)/I(\xi)$ (up to 21%). Distributions of the quantities ξ_1 and $\varepsilon(\xi_1)$ within the considered range of the parameters γ/d and τ are presented in Figs. 5 and 6a. They show that the intensity of the radiation outgoing from the medium is underestimated.

Within the ranges specified, the accuracy of Eq. (5) can be improved to 14.5% by changing the numerical coefficient in the radical

$$\xi_2(\gamma/d, \tau) = \frac{1}{\sqrt{1 + 0.1803\tau\gamma/d}}\,. \tag{7}$$

The distribution of the intensity error $\varepsilon(\xi_2)$ resulting from calculations of ξ by Eq. (7) is presented in Fig. 6b. In this case, the character of the error is somewhat changed. Whereas in the previous case the intensity of the outgoing radiation was only underestimated, now regions appear within which the intensity is overestimated. Nevertheless, although the error decreased by a factor of 1.5, it still remains considerable.

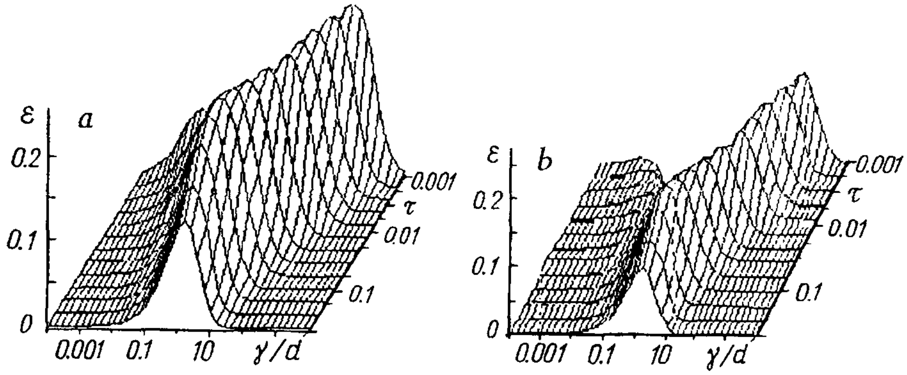

Fig. 6. Distribution of the intensity error emerging in computations of $\xi(\gamma/d, \tau)$ by Eq. (6) (a), $\xi_{max} = 0.21$ and by Eq. (7) (b), $\xi_{max} = 0.145$.

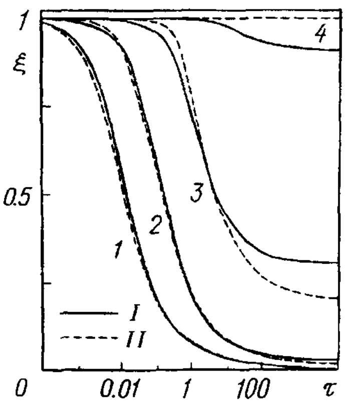

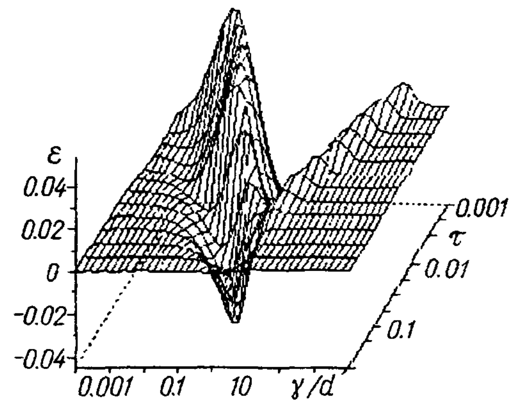

Fig. 7. Dependence of the correction factor ξ on the optical thickness τ for $\gamma/d = 0.001$ (1), 0.01 (2), 0.1 (3), and 0.5 (4); *I*, exact solution and *II*, approximating formula (8).

Fig. 8. Distribution of the intensity error emerging in computation of $\xi(\gamma/d, \tau)$ by Eq. (8), $\xi_{max} = 0.0452$.

An analysis of the distribution of the correction factor and intensity errors made it possible to offer a different relatively simple formula for calculation of the correction coefficient $\xi(\gamma/d, \tau)$:

$$\xi_3(\gamma/d, \tau) = \begin{cases} \alpha, & \alpha \le 1, \\ 1, & \alpha \ge 1, \end{cases} \tag{8}$$

$$\alpha = 2\frac{\gamma}{d}\left[1 - \exp\left(-0.05635\tau/(\gamma/d)^2\right)\right] + 1/\sqrt{1 + 0.2254\tau\gamma/d}\,.$$

Its use reduces the error in calculations of the radiation intensity by a factor of five compared to the original formula (6). It should be noted that $\varepsilon(\xi_3)$ does not exceed 4.52% over the entire range of the parameters γ/d and τ. The character of variation of the quantity ξ is illustrated by Fig. 7. An analysis of the intensity error distribution (Fig. 8) shows that the use of formula (8) can lead to both under- and overestimation of the intensity of radiation outgoing from the medium, but no more than by 4.52%. We point out that for approximately 40% of the range considered the error ξ_3 does not exceed 1%.

It should also be pointed out that if one sets $\xi_3 = \alpha$ in Eq. (8), $\xi_3 > 1$ for $\gamma/d > 0.1$ and $\tau > 10$, but the absolute magnitude of the intensity error $\varepsilon(\xi_3)$ does not increase, since for these values of the parameters the optimal thickness of the medium within the lineshape always exceeds three, and the selectivity effect decreases, and therefore, no substantial changes in the lineshape-averaged intensity of the outgoing radiation are observed upon further increase in the effective optical thickness of the medium.

Further attempts to decrease the magnitude of the error within the considered wide range of the parameters γ/d and τ by means of a different approximating formula were not successful. The complexity of computation and the CPU time for calculations by other formulas exceeded the computational expenses for simple interpolation of tabulated values.

However, results of these investigations have shown that one can develop relatively simple approximating formulas ($\varepsilon < 1\%$) for cases when the quantities γ/d and τ vary by an order of magnitude. However, in our opinion, for these ranges of variations of the parameters γ/d and τ interpolation of tabulated accurate values of the correction factor $\xi(\gamma/d, \tau)$ is more convenient.

Conclusion. Formula (8) makes it possible to take into account the fine structure of the absorption line in calculations of the effective absorption coefficient for nonscattering media. When propagation of radiation is calculated in scattering media within the range of changes of the parameters of the fine structure of the line within which the Schuster number, by varying over the lineshape, leads to substantial changes in the effective optical thickness τ_0, the use of Eq. (8) leads to large errors (of an order of 40%) in calculations of the radiation intensity of a selective medium. To reduce this error, one should likely introduce into Eq. (8) a correcting factor that would account for the effect of scattering processes on the lineshape-averaged absorption coefficient. In this case, the effective absorption coefficient of a selective component of a scattering medium within a finite spectral range can be presented as follows:

$$\chi = \frac{s}{d} \xi (\gamma/d, \tau_a) \vartheta (\gamma/d, \tau_a, \mathrm{Sc_a}) ,$$

where $\vartheta(\gamma/d, \tau_a, \mathrm{Sc_a})$ is the correcting factor accounting for the effect of scattering on the lineshape of the outgoing radiation, which equals unity at $\mathrm{Sc_a} = 0$.

NOTATION

$I(m, l)$, radiation intensity at point l along the direction $m = \cos\theta$ (θ being the angle between the direction of propagation of radiation and the Ox axis); χ and σ, absorption and scattering coefficients of the medium; a, doubled fraction of radiation backscattered by a unit volume of the medium; L, geometrical thickness of the layer; s, strength of absorption line; γ, halfwidth of absorption line; d, interline spacing; z, distance from the line center; ξ, correction factor accounting for radiation lineshape. Subscript: a, absorption-averaged values.

REFERENCES

1. G. A. Damoto and W. C. Wang, *J. Heat Transfer*, **8**, No. 2, 385-390 (1974).
2. I. A. Vasilieva, *JQSRT*, **33**, No. 3, 171-178 (1986).
3. D. G. Goodwin and J. L. Ebert, *JQSRT*, **37**, No. 5, 501-508 (1987).
4. W. Malkmus, *JQSRT*, **40**, No.3, 201-204 (1988).
5. W. A. Fiveland, *J. Heat Transfer*, **106**, No. 3, 699-706 (1984).
6. L. S. Rothman, *JQSRT*, **48**, No. 5/6, 469-507 (1992).
7. C. B. Ludwig, W. Malkmus, and A. L. Thompson, *Handbook on Infrared Radiation from Combustion Gases*, NASA SP-3080, Huntsville (1973).
8. R. M. Goody and V. L. Young, *Atmospheric Radiation*, Oxford (1989).
9. P. Riviere, S. Langlois, A. Soufiani, and J. Taine, *JQSRT*, **53**, No. 2, 221-234 (1995).
10. M. Modest, *J. Heat Transfer*, **113**, 650-656 (1991).
11. M. K. Denison and B. W. Webb, *JQSRT*, **50**, No. 7, 499-510 (1993).
12. M. L. German, Effects of Optical Properties of Two-Phase Medium and Boundary Surface on Radiative Heat Transfer in Combustion Chambers, *Author's Abstract of Candidate's Dissertation in the Physicomathematical Sciences*, Minsk (1993).
13. K. S. Adzerikho, E. F. Nogotov, and V. P. Trofimov, *Radiative Heat Transfer in Two-Phase Media* [in Russian], Minsk (1987).